Received: 14 May 2019 | Accepted: 16 May 2019

DOI: 10.1002/pamm.201900150

Topology Optimization with Isogeometric Analysis and Phase Field Modeling

Ingo Muench[1,*], **Markus Klassen**[2], and **Werner Wagner**[1]

[1] KIT, Kaiserstr. 12, D-76131 Karlsruhe
[2] RWTH Aachen, Mies-van-der-Rohe-Str. 1, D-52074 Aachen

We use a Phase Field Model (PFM) for the evolution of load-bearing structures on base of the equivalent stress criterion. Similar to Evolutionary Structural Optimization, the equivalent stress from all integration points is collected to evaluate a threshold. The approach couples density and stiffness to the phase field variable. The topology evolves from homogeneously filled regions by nucleation of holes. In numerical examples we compare results using standard Finite Elements (FEM) and Isogeometric Analysis (IGA), respectively. Latter allows for higher continuity between elements, which is essential to avoid the well-known mesh-pinning effect.

1 Introduction

For the comprehensive optimization of frame structures in civil engineering, we pursue a high level of automatization and decompose the task into two stages. First, the phase field model generates a load bearing topology with almost homogeneous von Mises stress. Then, monolithic shape and size optimization, with help of metaheuristic algorithms, is performed [1, 2]. The use of different optimization algorithms is adjusted by the different requirements of each stage. The phase field model determines the relevant characteristics of the structure such as the number of beams and position of nodes. Then, image processing algorithms transform the phase field results into a simplified beam model for the next step of optimization [3, 4].

2 The phase field model

To compare results between standard FEM and IGA, we restrict ourself to linear strain $\varepsilon = \mathrm{SymGrad}[u]$ as proposed in [5, 6]. However, we refer to [7, 8], if Green or Cosserat strain is of interest. The phase field variable φ defines the density ρ_φ and strain stiffness $\mathbb{C}_\varphi$ of the substance, where ρ_0 and $\mathbb{C}_0$ represent the material phase and $f(\varphi) \to 0$ yields void:

$$f(\varphi) = \frac{\mathrm{e}^{\alpha\,\varphi}}{\mathrm{e}^{\alpha\,\varphi}+1}\,,\; f \in [0,1]\;, \quad \rho_\varphi = f(\varphi)\,\rho_0\,, \quad \mathbb{C}_\varphi = f(\varphi)\,\mathbb{C}_0\,. \tag{1}$$

The transition from void to material is allocated by $\varphi \in [-1, 1]$. We recommend to use $\alpha = 14$ to obtain $f(-1) \approx 1 \cdot 10^{-6}$, and $f(1) \approx 1$. The inner energy considers a double-well potential ψ_w, an interface term ψ_g and a strain energy ψ_s according to

$$\Pi_\mathrm{i} = \int_{\mathcal{B}} \underbrace{[\psi_\mathrm{w} + \psi_\mathrm{g} + \psi_\mathrm{s}]}_{\psi}\,\mathrm{d}V\,,\; \psi_\mathrm{w} = \varphi^6 - \varphi^4 - \varphi^2 + 1\,,\; \psi_\mathrm{g} = \frac{1}{2}\,L_c\,||\mathrm{Grad}[\varphi]||^2\,,\; \psi_\mathrm{s} = \frac{1}{2}\,f(\varphi)\,\varepsilon : \mathbb{C}_0 : \varepsilon\,, \tag{2}$$

within the design space $\mathcal{B}$. Let us define the stress σ as well as phase field sensitivities η and ξ according to

$$\sigma = \frac{\partial\psi}{\partial\varepsilon} = f(\varphi)\,\mathbb{C}_0 : \varepsilon\,,\; \eta = \frac{\partial\psi}{\partial\varphi} = \frac{1}{2}\,f'(\varphi)\,\sigma : \varepsilon + 6\,\varphi^5 - 4\,\varphi^3 - 2\,\varphi\,,\; \xi = \frac{\partial\psi}{\partial\mathrm{Grad}[\varphi]} = L_c\,\mathrm{Grad}[\varphi]. \tag{3}$$

Our objective function F contains the threshold $\bar\sigma_V$ evaluated from the stress field on base of the desired filling level $\widehat{K}$

$$F = \int_{\mathcal{B}} \underbrace{\gamma_s\,\frac{\bar\sigma_V(\widehat{K}) - \sigma_V}{\bar\sigma_V(\widehat{K})}}_{=:\gamma}\,\varphi\;\mathrm{d}V \;\to\; \min \text{ w.r.t. } u\,,\,\varphi\,, \quad K = \frac{\int_{\mathcal{B}} f(\varphi)\;\mathrm{d}V}{\int_{\mathcal{B}}\;\mathrm{d}V} \;\in [0,1] \;\to\; \widehat{K}\,. \tag{4}$$

The external work accounts for volume forces $\rho_\varphi\,b$ and the source of material γ as defined in Eq.4. Similar to mechanical tractions t, let us consider injection or rejection of material y through the surface $\partial\mathcal{B}$ of the design space $\mathcal{B}$

$$\Pi_\mathrm{a} = \int_{\mathcal{B}} [\rho_\varphi\,b\cdot u + \gamma\,\varphi]\,\mathrm{d}V + \int_{\partial\mathcal{B}} [t\cdot u + y\,\varphi]\,\mathrm{d}A\,. \tag{5}$$

* Corresponding author: e-mail ingo.muench@kit.edu, phone +49 721 608 42289, fax +49 721 608 46015

The principle of virtual work yields $\mathrm{Div}\,\sigma + f\,\rho_0\,b = 0$. The phase field balance follows Allen and Cahn [9] yielding $\eta - \mathrm{Div}\,\xi - f'\,\rho_0\,b\cdot u + \gamma + \beta\,\dot{\varphi} = 0$. The Newton-Raphson scheme with backward Euler time integration solves

$$G = \int_{\mathcal{B}} \left[(\mathrm{Div}\,\sigma + f\rho_0\,b)\cdot\delta u + (\eta - \mathrm{Div}\xi + f'\rho_0\,b\cdot u + \gamma + \beta\,\dot{\varphi})\,\delta\varphi\right] \mathrm{d}V\,. \tag{6}$$

3 Numerical examples

Our examples consider $E = 1000$, $\nu = 0.3$ and parameters $\gamma_s = 5$, $L_c = 0.01$. In Fig.1a we seek the topology of a porch roof loaded by $F = 1$ with filling level $\widehat{K} = 0.1$. The performance of 200 finite elements using quadratic Ansatz functions are compared to 200 IGA cells using second order basis functions. This yields 2501 DOF for FEM but only 748 DOF for IGA. More details concerning phase field modeling with IGA is given in [10]. The optimized frameworks in Fig.1b show the 2-bar and the 4-bar roof. The PFM should be able to suggest both topologies. However, according to the rough mesh, FEM and

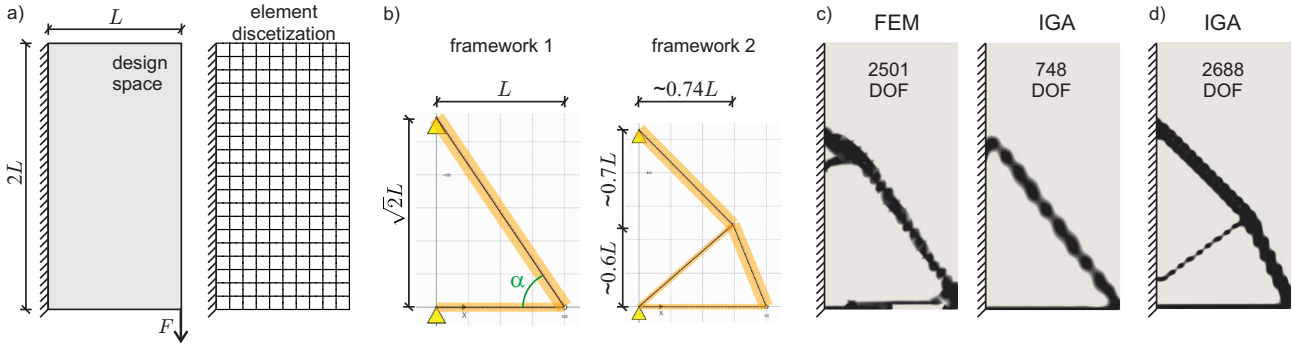

Fig. 1: a) Design space, boundary conditions, loading and element discretization of the example. b) Optimized frameworks with different topologies. c) Numerical results for FEM and IGA analysis yielding the 2-bar topology. d) IGA solution with 4-bar topology.

IGA evolve the 2-bar solution only, see Fig.1b. Nevertheless, with IGA we do not observe pronounced mesh pinning as for FEM. Next, we consider 800 cells for IGA to obtain 2688 DOF, which almost corresponds to FEM analysis. Now, depending on the parameter L_c, we obtain the 2-bar or the 4-bar solution as shown in Fig.1d.

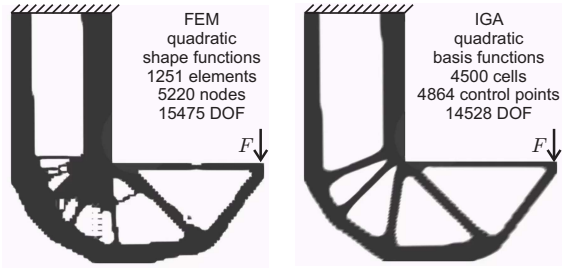

Fig. 2: Final state of the PFM evolution process for the L-bracket problem as suggested by Duysinx & Bendsøe.

Our second example investigates the L-bracket problem for $\widehat{K} = 0.4$. Obviously, the FEM analysis does not evolve a meaningful topology due to intense mesh-pinning, see Fig. 2. The IGA can consider more cells to obtain the same number of DOF as in the FEM analysis.

4 Conclusions

The PFM by IGA benefits from the larger number of cells and the higher continuity of the stress field for the same number of DOF compared to standard FEM. Mesh-pinning effects, as observed in standard FEM, do not interfere the evolving topology with IGA. However, the resolution of cells used for IGA influences the spectrum of available topologies.

References

[1] A. Keller, I. Muench, W. Wagner, Proceedings of the 7th GACM Colloquium on Computational Mechanics, 395-398 (2017).
[2] A. Keller, I. Muench, W. Wagner, Proc. Appl. Math. Mech. **17**, 743-744 (2017).
[3] A. Keller, I. Muench, W. Wagner, Form- und Systemoptimierung von Rahmentragwerken, in J. Schneider, N. Kiziltoprak (eds.) Forschungskolloquium 2018 Grasellenbach, Baustatik Baupraxis e.V., Springer Vieweg, 39-41 (2018).
[4] A. Keller, I. Muench, W. Wagner: Double-stage optimization of frame structures, Proc. Appl. Math. Mech. **18**, 1-2 (2018).
[5] I. Muench, Ch. Gierden, W. Wagner: A phase field model for stress based evol. of load-bearing struct., IJNME **115**, 1580-1600 (2018).
[6] I. Muench, in F.A. Radu, K. Kumar, I. Berre, J.M. Nordbotten, I.S. Pop (eds.) Numerical Mathematics and Advanced Applications - ENUMATH 2017, Lecture Notes in Computational Science and Engineering 126, Springer, 335-343 (2018).
[7] I. Muench, A. Keller: Evolution of structures with homogeneous equivalent stress, Proc. Appl. Math. Mech. **18**, 1-2 (2018).
[8] I. Muench: Structural optimization with Cosserat phase field modeling, Oberwolfach Reports 20, 49-53 (2018).
[9] J. Cahn, S. Allen, Journal de Physicque Colloques **38**, 51–54 (1977).
[10] M. Klassen, I. Muench, S. Klinkel: Phase field modeling with IGA and FEM: Error surveillance in the transition zone, to appear in Proc. Appl. Math. Mech.

